JOURNAL OF VIROLOGY, May 1982, p. 432–439
0022-538X/82/050432-08$02.00/0

Vol. 42, No. 2

Sequence Relationships Between the Genome and the Intracellular RNA Species 1, 3, 6, and 7 of Mouse Hepatitis Virus Strain A59

WILLY J. M. SPAAN,* PETER J. M. ROTTIER, MARIAN C. HORZINEK, AND BERNARD A. M. VAN DER ZEIJST

Institute of Virology, Veterinary Faculty, State University, 3508 TD Utrecht, The Netherlands

Received 30 September 1981/Accepted 22 December 1981

We have shown by T_1 oligonucleotide fingerprinting that the genome of mouse hepatitis virus strain A59 and its intracellular RNA 1 have identical fingerprints and that RNA 1 and the subgenomic RNAs 3, 6, and 7 contain common sequences. To localize the homologous region between the RNAs, we compared fingerprints of the 3′ terminus of the genome with those of RNA 7. The genome was partially degraded with alkali, and polyadenylate-containing fragments were purified by oligodeoxythymidylate-cellulose chromatography. The fragments were size fractionated by agarose-urea gel electrophoresis, and two pools, x and z, containing 3′-derived fragments of the genome with apparent molecular weights of 0.1×10^6 to 0.14×10^6 and 0.6×10^6 to 0.8×10^6, respectively, were further analyzed by RNase T_1 oligonucleotide fingerprinting. Comparison of the fingerprints of RNAs 6 and 7 with those of pools x and z showed that these subgenomic RNAs extend inwards from the 3′ terminus of the genome. The RNA fragments present in pool z were on average slightly larger than RNA 7 as confirmed by the presence in pool z of T_1 oligonucleotide spots specific for RNA 6 but not present in RNA 7. However, two large oligonucleotide spots derived from RNA 7, which were also present in RNAs 1, 3, and 6 and in the virion RNA, were not found in the T_1 oligonucleotide map of pool z. A possible explanation is that the two spots were derived from a leader sequence. The results of UV transcription mapping experiments (L. Jacobs, W. J. M. Spaan, M. C. Horzinek, and B. A. M. van der Zeijst, J. Virol. 39:401–406, 1981) excluded the possibility that such a leader sequence arises by splicing from a larger precursor molecule, but either a virus-specific RNA primer molecule for the synthesis of mRNAs or an RNA polymerase jumping mechanism could explain the presence of a leader sequence.

Five or six subgenomic RNAs are involved in the replication of coronaviruses, a group of enveloped positive-stranded RNA viruses (1, 13–16). From their polyadenylation and their presence in polyribosomes, it is evident that these RNAs are mRNAs; moreover, three of the murine coronavirus subgenomic RNAs have been translated into proteins in a cell-free system or in *Xenopus laevis* oocytes (11, 12). Since the total molecular mass of the subgenomic mRNAs is almost twice that of the genome, sequence homologies must exist between these mRNAs. We previously presented a speculative model in which the genomic and subgenomic RNAs of mouse hepatitis virus strain A59 (MHV-A59) were supposed to share a homologous region of 0.6×10^6 daltons at their 3′ termini (13). It was also assumed that the internal initiation sites for protein synthesis on the genome and the subgenomic RNAs were not accessible; in each mRNA, only the 5′-terminal region not present in the next smaller RNA would be translated (13).

Stern and Kennedy (14, 15) demonstrated that the five subgenomic mRNAs and the gneome of the avian coronavirus infectious bronchitis virus indeed form a "nested set" of RNAs sharing a common 3′ region. Weiss and Leibowitz (18) have shown by hybridization of short cDNA probes specific to the 3′ end of genomic RNA to all subgenomic RNAs that the genome and the subgenomic RNAs share at least a number of 3′ sequences. Similarly, Cheley et al. (1) were able to hybridize all subgenomic RNAs of MHV-A59 with cDNA to RNA 7. However, with this approach, one cannot exclude that the subgenomic RNAs contain additional sequences which are homologous to 5′-proximal sequences of the genome.

Here we present RNase T_1 oligonucleotide

fingerprints of the genome and of intracellular RNAs 1, 3, 6, and 7 which confirm that the MHV-A59-specific RNAs also form a nested set. We also wanted to compare the RNase T_1 oligonucleotide fingerprints of RNAs 6 and 7 with those of fragments derived from the 3′ end of the genome. Not only was this important for ascertaining that the subgenomic mRNAs extend inwards from the 3′ terminus of the genome, but it also gave more information on the transcription mechanism leading to the synthesis of these mRNAs. By using UV transcription mapping, we have recently shown that the subgenomic mRNAs are transcribed by independent initiation rather than by processing of full-length positive-stranded RNA molecules (5). We could not exclude, however, the presence of short 5′-terminal sequences which are common to all subgenomic RNAs and are, e.g., derived by a polymerase jumping mechanism. If certain characteristic spots in the RNase T_1 oligonucleotide fingerprints of the virus-specific RNAs would be derived from such short 5′-terminal sequences, comparison of the fingerprints of RNAs 6 and 7 with those of the 3′ terminus of the genome might resolve this problem, since these spots would not be present in the T_1 oligonucleotide fingerprints of the 3′ end of the genome.

We compare our data with those reported very recently by Lai et al. (6) and Leibowitz et al. (9).

MATERIALS AND METHODS

Actinomycin D was purchased from Serva, Heidelberg, Germany. Carrier-free $^{32}P_i$, [5′-^{32}P]cytidine 3′,5′-bisphosphate (pCp) (2,000 to 3,000 Ci/mmol), and [γ-^{32}P]ATP (>2,000 Ci/mmol) were obtained from the Radiochemical Centre, Amersham, England. Rabbit liver glycogen was purchased from BDH Biochemicals Ltd., Poole, England. It was further purified as described by Stern and Kennedy (15). Oligodeoxythymidylate [oligo(dT)]-cellulose (type 7) and polyguanylic acid [poly(G)] were purchased from P-L Biochemicals Inc., Milwaukee, Wis. Polypropylene tubes were used in the experiments in which RNA was involved; they were pretreated with a 5% solution in carbon tetrachloride of dimethyldichlorosilane, rinsed well with distilled water, and autoclaved.

Enzymes. T_4 RNA ligase, T_4 polynucleotide kinase, and bacterial alkaline phosphatase were purchased from P-L Biochemicals. Bacterial alkaline phosphatase was further purified and treated with diethylpyrocarbonate as described by Pedersen and Haseltine (10). RNase T_1 was purchased from Calbiochem, La Jolla, Calif.

Cells and virus. Virus stocks of plaque-purified MHV-A59, propagated in Sac(−) cells, were prepared as described previously (13).

^{32}P labeling of virus-specific intracellular RNAs and virion RNA. Two 150-cm^2 T flasks each containing approximately 4×10^7 Sac(−) cells were infected with MHV-A59 at a multiplicity of infection of 20. Inocula were in 3 ml of Dulbecco-modified Eagle medium (DMEM)–3% fetal calf serum (FCS). After an adsorption period of 1 h at 37°C, the inocula were removed, and the cells were washed once with salt solution A (137 mM NaCl, 4 mM KCl, 1.6 mM $CaCl_2$, 1 mM $MgCl_2$, 23.8 mM $NaHCO_3$, 10 mM glucose, 20 mg of phenol red per liter, pH 7.2). Ten milliliters of phosphate-deficient DMEM buffered with 20 mM HEPES (*N*-2-hydroxyethylpiperazine-*N*′-2-ethanesulfonic acid)–KOH at pH 7.2 and supplemented with 5% dialyzed FCS was added. At 4 h postinfection, the culture fluid was replaced with 10 ml of the same medium supplemented with 1 μg of actinomycin D per ml, and 1 h later, 200 μCi of $^{32}P_i$ per ml was added. At 8 h postinfection, the cells were lysed, and RNA was phenol extracted as described previously (13). At the same time, the infectious culture fluid was clarified, and the virus was precipitated with polyethylene glycol 6000 and purified in a sucrose gradient as described previously (13). Sucrose gradient fractions were Cerenkov counted, and the fractions containing the virus peak were pooled. Virion RNA was phenol extracted after incubation with sodium dodecyl sulfate (SDS) and proteinase K as described previously (13).

Selection of poly(A)-containing RNAs. Virus-specific intracellular RNAs extracted from the two 150-cm^2 T flasks were recovered by ethanol precipitation, dried in vacuo over $CaCl_2$, dissolved in 500 μl of high-salt-binding buffer, and chromatographed on an oligo(dT)-cellulose column as described before (13).

Preparative agarose gel electrophoresis. The ^{32}P-labeled poly(A)$^+$ RNAs from infected cells were dissolved in 150 μl of 10 mM sodium phosphate (pH 7.0) containing 1 mM EDTA, 0.25% SDS, 6 M urea, and 10 μg of bromophenol blue per ml. The solution was heated for 5 min at 56°C, rapidly cooled on ice, placed in a slot (40 by 2 mm) of a horizontal 1% agarose–6 M urea slab gel (19 by 19 by 0.2 cm), and electrophoresed for 5 to 6 h at 200 V. RNA bands were located by autoradiography of the wet gel, excised, and kept at −20°C.

Elution of RNA from gel slices. RNA was eluted from gel slices by the method of Langridge et al. (8). Briefly, the gel slices were melted for 5 min at 65°C, and equal volumes of 1-butanol saturated with distilled water containing 36.7 g of cetyltrimethylammonium bromide (CTAB) per liter and of distilled water saturated with 1-butanol were added. The phases were separated by centrifugation (10,000 × *g* for 5 min). The aqueous phase was extracted once more with CTAB-containing water-saturated 1-butanol. The CTAB salts of the RNAs were twice extracted from the combined butanol phases with 0.25 volume of 0.2 M NaCl. Finally, the CTAB was extracted from the 0.2 M NaCl-containing aqueous phases with chloroform, and the RNA was precipitated by the addition of 2 volumes of ethanol in the presence of 0.1 M sodium acetate (pH 5.2) and 20 μg of *Escherichia coli* carrier tRNA per ml.

Analytical agarose gel electrophoresis. RNA samples were denatured with glyoxal and dimethyl sulfoxide and analyzed by electrophoresis in a 1% agarose–6 M urea horizontal slab gel as described previously (13).

RNase T_1 fingerprinting. RNase T_1 fingerprinting was first described by De Wachter and Fiers (3). We used the modification of the conditions for the RNA

digestion and two-dimensional gel electrophoresis described by Clewley et al. (2), with some additional modifications. After digestion with RNase T_1, the digest was mixed with solid urea to give 20 μl, with a final concentration of 6 M urea. Subsequently, 10 μl of a solution containing 6 M urea, 50% (wt/vol) sucrose, 0.2% xylene cyanol FF, 0.2% bromophenol blue, and 15 mg of *E. coli* tRNA per ml was added. The mixture was heated to 56°C for 5 min, rapidly cooled on ice, and placed in a slot of the 10% (wt/vol) (pH 3.3) first-dimension polyacrylamide gel. Electrophoresis buffer consisted of 6 M deionized urea adjusted to pH 3.3 with saturated citric acid. Electrophoresis was at 1,000 V and 40 mA for 5 to 8 h at 4°C. After electrophoresis, a gel strip (24 by 1 cm) was excised for use in the second dimension. This strip was positioned between two glass plates, and the gel for the second dimension containing 21.8% (wt/vol) acrylamide, 0.7% bisacrylamide, 100 mM Tris-borate (pH 8.3), and 2.5 mM EDTA was poured around it. Electrophoresis in the second dimension was at 600 V and 50 mA per gel for 16 to 24 h at 4°C. The electrophoresis buffer for the second dimension consisted of 100 mM Tris-borate (pH 8.3) containing 2.5 mM EDTA. After electrophoresis, one glass plate was removed, and the gel was covered with a polyethylene film (Saran Wrap). Autoradiography was carried out at 4°C by exposure of the gel to Kodak XR film, using an intensifier screen (Du Pont Lightning Plus).

Preparation of virion RNA. Two roller-bottle cultures of Sac(−) cells (2×10^8 cells per bottle) were infected with MHV-A59 at 2 PFU per cell as described previously (13). The infectious culture fluid was harvested at 19 h postinfection and clarified, and the virus was precipitated with polyethylene glycol 6000 and purified in a sucrose gradient (13). Genomic RNA was isolated from the sucrose gradient-purified virus preparation as follows. Gradient material (1.5 ml) was mixed with 1.5 ml of dissociation buffer (0.05 M Tris-hydrochloride [pH 8.2], 0.1 M NaCl, 0.01 M EDTA, 2% sodium lauryl sarcosinate, 1% sodium deoxycholate, 2% sodium *p*-aminosalicylate, 0.5% disodium triisopropylnaphthalene sulfonate). Then 0.03 g of solid SDS and 3 g of CsCl were added. After the salts had dissolved, the sample was heated at 65°C for 5 min. It was then layered onto 1.2 ml of 5.7 M CsCl in 0.02 M Tris-hydrochloride (pH 8.2)–0.1 M EDTA and centrifuged for 19 h at 35,000 rpm and 20°C in a Beckman SW50.1 rotor. The RNA pellet was dissolved in 200 μl of water, and the RNA was precipitated by the addition of 2 volumes of ethanol in the presence of 0.1 M sodium acetate (pH 5.2).

Fragmentation of virion RNA with alkali. Fifty micrograms of virion RNA was dissolved in 100 μl of TE buffer (20 mM Tris, pH 7.4, 2 mM EDTA). An equal volume of freshly prepared 2 M Na_2CO_3 was added, and the mixture was incubated for 2 min at 25°C. The reaction was terminated by neutralization with 16 μl of glacial acetic acid. Immediately thereafter, the solution was made 0.3 M in sodium acetate (pH 5.2). RNA was precipitated by the addition of 2 volumes of ethanol. The mixture was kept at −20°C for at least 16 h before the RNA was collected by centrifugation.

3′-End labeling of RNA. End labeling of RNA was performed by the procedure of England and Uhlenbeck (4). Ethanol-precipitated fragments of virion RNA were dried in vacuo over $CaCl_2$ and dissolved in 20 μl of water. This solution was transferred to a tube containing 90 μCi of lyophilized [5′-^{32}P]pCp. Then 10 μl of a buffer containing 150 mM HEPES (pH 8.0), 9 mM dithiothreitol, 30 mM $MgCl_2$, 15 μM ATP, and 14 U of RNA ligase was added. After incubation for 18 h at 4°C, 200 μl of oligo(dT)-cellulose high-salt-binding buffer was added, and the mixture was applied to an oligo(dT)-cellulose column. After the column was extensively washed with high-salt-binding buffer, the bound material was eluted in 0.5 ml of 10 mM Tris-hydrochloride, pH 7.5. The eluate was adjusted to 0.3 M sodium acetate, and 50 μg of glycogen carrier was added. RNA was precipitated with 2 volumes of ethanol at −20°C for at least 16 h.

Size selection of poly(A)-containing fragments of the genome. The 3′-end-labeled poly(A)-containing fragments of the genome were ethanol precipitated, dried in vacuo over $CaCl_2$, and dissolved in 50 μl of 10 mM sodium phosphate (pH 7.0) containing 1 mM EDTA, 0.25% SDS, 6 M urea, and 10 μg of bromophenol blue per ml. The fragments were separated in an agarose-urea gel, using the conditions described above for the preparative separation of the virus-specific intracellular RNAs. After electrophoresis, the gel was cut into transversal slices (3 mm) which were Cerenkov counted.

Elution of RNA fragments from gel slices. The gel slices were melted for 5 min at 65°C, and an equal volume of phenol-chloroform (1:1) saturated with TES buffer (0.02 M Tris-hydrochloride, 1 mM EDTA, 0.1 M NaCl, pH 7.4) and supplemented with 0.1% 8-hydroxyquinoline was added. After separation of the phases, an equal volume of double-concentrated oligo(dT)-cellulose high-salt buffer was added to the water phase, and the mixture was applied to an oligo(dT)-cellulose column. The bound material was eluted with 0.5 ml of 10 mM Tris-hydrochloride (pH 7.5). The eluate was adjusted to 0.3 M sodium acetate (pH 5.2), and 50 μg of glycogen was added before RNA was ethanol precipitated as described above.

RNase T_1 fingerprinting of 3′-derived fragments of the genome. After ethanol precipitation, the purified RNA fragments were dried in vacuo over $CaCl_2$ and dissolved in 20 μl of 20 mM Tris-hydrochloride (pH 8.0)–2 mM EDTA. Then 5 μl of an RNase T_1 digestion mixture containing 5 U of RNase T_1, 2.5 mU of bacterial alkaline phosphatase, and 100 ng of poly(G) in 20 mM Tris-hydrochloride (pH 8.0)–2 mM EDTA was added. The samples were incubated for 60 min at 37°C. After this period, the RNase T_1-resistant oligonucleotides were 5′ end labeled with $^{32}P_i$ by the addition of 40 μl of a polynucleotide kinase reaction mixture of the following composition: 10 mM potassium phosphate (pH 9.5), 10 mM magnesium acetate, 5 mM dithiothreitol, 2 μM [γ-^{32}P]ATP, and 50 U of polynucleotide kinase per ml. The samples were incubated for 2 h at 37°C before the reaction was terminated by the addition of 50 μl of 0.6 M ammonium acetate containing 2 mg of carrier *E. coli* tRNA per ml. The mixture was extracted with an equal volume of phenol saturated with 10 mM Tris-hydrochloride (pH 8.0), and the RNA was ethanol precipitated. The pellets containing the ^{32}P-labeled RNase T_1 oligonucleotides were washed twice with 70% ice-cold ethanol containing 50 mM NaCl and then dried in vacuo over $CaCl_2$. They were dissolved in 20 μl of TE buffer containing 6 M urea and fingerprinted as described above.

RESULTS

Isolation of ^{32}P-labeled virus-specific intracellular RNAs 1, 3, 6, and 7. To purify MHV-A59-specific intracellular RNAs for RNase T_1 oligonucleotide fingerprinting, ^{32}P-labeled virus-specific RNAs were isolated from infected Sac(−) cells by phenol extraction and ethanol precipitation. A poly(A)-containing fraction was prepared by oligo(dT)-cellulose chromatography. The virus-specific RNAs were separated in an agarose-urea gel. The position of each of the RNAs was determined by autoradiography of the wet gel, and bands corresponding to RNAs 1, 3, 6, and 7 were excised. The RNAs were eluted from the gel and concentrated by ethanol precipitation. Small samples of these RNA preparations were denatured with glyoxal-dimethyl sulfoxide and analyzed by electrophoresis in an agarose-urea gel. As shown in Fig. 1, pure preparations of RNAs 1, 3, and 7 were obtained, whereas RNA 6 was still slightly contaminated with RNA 7.

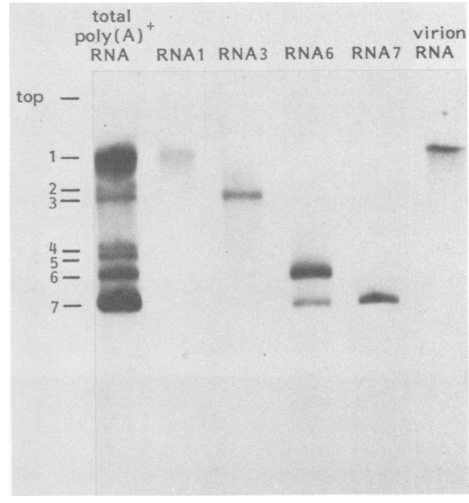

FIG. 1. Analysis of purified MHV-A59-specific intracellular RNAs and virion RNA. ^{32}P-labeled intracellular RNA was isolated at 8 h postinfection from infected cultures of Sac(−) cells, the poly(A)-containing fraction was isolated by oligo(dT)-cellulose chromatography and electrophoresed in a 1% agarose-6 M urea gel. RNA bands corresponding to RNAs 1, 3, 6, and 7 were excised from the gel, and RNA was eluted from the gel slices. Genomic RNA was extracted from purified virus. The RNAs that were denatured with glyoxal-dimethyl sulfoxide were electrophoresed in a 1% agarose-6 M urea gel. A sample of ^{32}P-labeled unfractionated poly(A)-containing RNA was run as a marker.

RNase T_1 oligonucleotide fingerprinting of genomic RNA and of RNAs 1, 3, 6, and 7. We used the method originally described by De Wachter and Fiers (3) to characterize and compare the MHV-A59-specific RNA species. This method consists of making fingerprints of the oligonucleotides that remain after complete digestion of the RNA with RNase T_1. Since denatured RNA 1 and virion RNA had the same mobility when electrophoresed in an agarose-urea gel (Fig. 1) (13), and since more than 90% of RNA 1 is present in EDTA-resistant, presumably ribonucleoprotein, particles (13), we assumed that RNA 1 is the intracellular form of the virion RNA. This assumption is supported by the identical RNase T_1 oligonucleotide fingerprints of the two RNAs (Fig. 2). To obtain more information about the sequence relationships among the virus-specific RNAs 1, 3, 6, and 7, we compared the fingerprints of these RNAs. As shown in Fig. 2, all oligonucleotide spots originating from RNA 7 were also present in RNA 6. This implies that RNA 6 (0.9×10^6 daltons) is a sequence extension of RNA 7 (0.6×10^6 daltons). A number of additional spots derived from this sequence extension were found in RNA 6. With the exception of one spot (Fig. 2, arrow) discussed below, the T_1 oligonucleotide spots from RNA 6 were contained within the fingerprint of RNA 3; on its turn, RNA 3 contained additional spots not found in RNA 6. All of the spots from RNA 3 were present in the fingerprint of RNA 1. Many additional spots were found in the T_1 oligonucleotide map of RNA 1; only a number of these spots are indicated in a schematic representation of the T_1 oligonucleotide maps of the RNAs (Fig. 2, arrowheads). Comparison of the fingerprints of RNAs 3, 6, and 7 showed that 37 of the larger, presumably characteristic, oligonucleotides (those beneath the position of the bromophenol blue tracker dye) were present in RNA 3 but not in RNA 6 (open spots). RNA 6 contained 18 spots, 8 of which (cross-hatched) were not found in RNA 7, which contained 10 spots (black). The overall conclusion of these experiments was that RNAs 3, 6, and 7 are indeed subgenomic RNAs and that they all share a region of the genome as long as and homologous to RNA 7.

Sequence relationship between the genome and RNA 7. Assuming that the homologous region in the RNAs would be localized at the 3′ terminus of the genome, we compared fingerprints of the 3′ region of the genome with those of RNA 7. For this purpose, the genome was partially degraded with alkali.The 3′-derived poly(A)-containing fragments possessing a free hydroxyl group were end labeled with T_4 RNA ligase and [5′-^{32}P]pCp, purified by oligo(dT)-cellulose chromatography, and size fractionated by agarose-urea gel electrophoresis. Transversal slices of the gel were counted to determine the distribution of the radioactivity among the fractions (Fig. 3), and fractions were pooled as indicated.

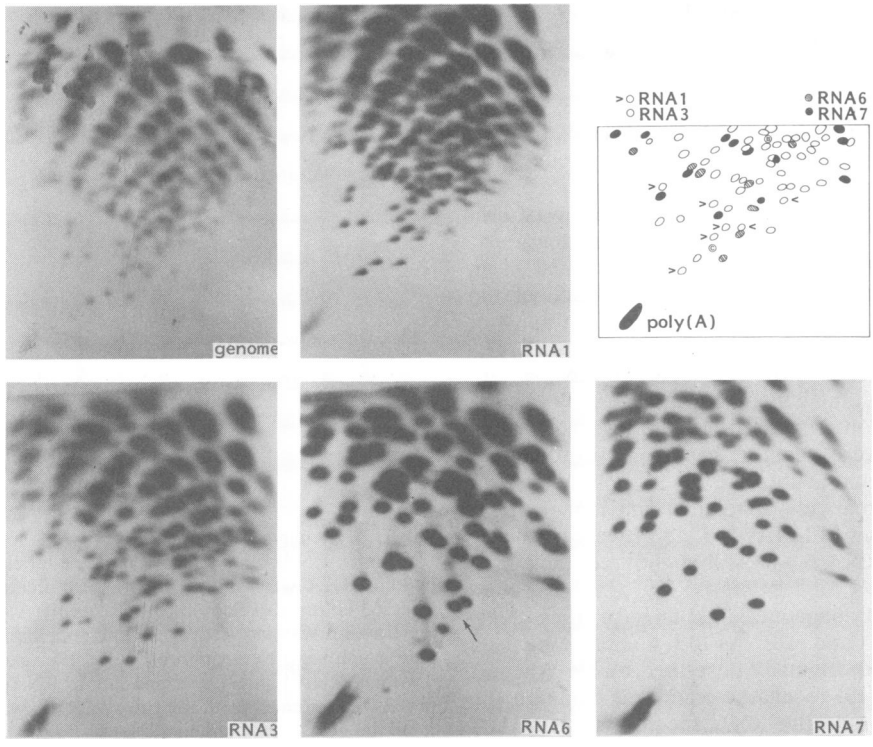

FIG. 2. RNase T_1 oligonucleotide fingerprints of the genome of MHV-A59 and the intracellular RNAs 1, 3, 6, and 7. ^{32}P-labeled intracellular RNA species 1, 3, 6, and 7 and genomic RNA were isolated as described in the legend to Fig. 1. The amount of label fingerprinted varied between 10^5 and 2×10^5 Cerenkov cpm. In these and subsequent fingerprints, electrophoresis was from left to right in the first dimension and from bottom to top in the second dimension. The data are summarized in a schematic drawing of the lower parts of the T_1 oligonucleotide fingerprints in which the positions of the xylene cyanol FF and bromophenol blue tracker dyes are indicated by C and B, respectively. In the scheme, the black dots indicate the RNase T_1 oligonucleotides present in RNA 7; the cross-hatched spots indicate the spots specific for RNA 6 compared with RNA 7; and the open spots indicate the extra oligonucleotides in RNA 3 compared with RNA 6. The open spots marked by arrowheads were specific for RNA 1. The significance of the spot in the fingerprint of RNA 6 marked with an arrow is discussed in the text.

Pools x and z were chosen for further analysis. They represented 3′-terminal sequences of the genome with apparent molecular weights of 0.1×10^6 to 0.14×10^6 and 0.6×10^6 to 0.8×10^6, respectively. The material present in these two pools was eluted from the gel and rechromatographed on oligo(dT)-cellulose columns to ascertain that only poly(A)-containing fragments were selected. Subsequently, the RNA fragments from pools x and z were digested with RNase T_1, the 5′ termini of the resulting RNase T_1 oligonucleotides were kinase labeled, and fingerprints were made. Figure 4 shows the results of this experiment. As expected, all RNase T_1 oligonucleotide spots from pool x were present in pool z. Pool z contained a number of additional spots representing the sequence extensions of pool x. All RNase T_1 oligonucleotide spots from pool x were present in RNA 7 (Fig. 2 and 4). Comparison of the fingerprints of RNA 7 and pool z showed that with the exception of two spots (Fig. 4, asterisks), all of the RNase T_1 oligonucleotide spots from RNA 7 were also present in pool z. This was also confirmed by the fingerprint of a mixture of the RNase T_1 oligonucleotides of pool z and RNA 7 (Fig. 4). Pool z contained several spots which were not present in RNA 7 but which were found in RNA 6. The spots, present in pool z but not in pool x, are indicated with z in a scheme of the fingerprint from RNA 6, whereas the spots present in pool x are indicated with x in this scheme (Fig. 4). From these results it can be concluded that RNA 7 is homologous to the 3′-terminal region of the genome. Moreover, by comparing the fingerprints of RNA 6, RNA 7, pool x, and pool z, we were able to map a number of RNase T_1 oligonucleotide spots on the genome. The spots marked x in the scheme in Fig. 4 were derived from the extreme 3′ end of the genome and,

therefore, also of all other RNAs. The open spots marked z were from the 5'-proximal end of RNA 7, whereas the cross-hatched spots marked z were derived from the sequence of RNA 6 bordering, but not present in, RNA 7.

A few minor spots in the fingerprint from pool z were not present in RNAs 6 and 7 (Fig. 4). These spots did not correspond to any of the T_1 oligonucleotide spots present in the fingerprint from the genome. Therefore, we believe that they may have resulted from experimental artifacts.

The most surprising finding of this study was that although the RNA fragments present in pool z had on average a slightly greater molecular weight than RNA 7, as was confirmed by the fact that the fingerprint of pool z contained a number of oligonucleotide spots which were specific for RNA 6, nevertheless two of the RNA 7-specific spots (Fig. 4, asterisks) were not present in the fingerprint of pool z. A possible explanation is discussed below.

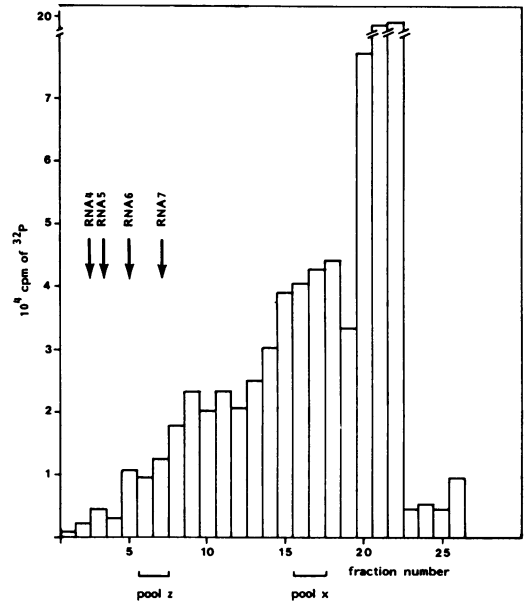

FIG. 3. Size fractionation by agarose-urea gel electrophoresis of 3'-derived fragments of the genome of MHV-A59. Genomic RNA was isolated from purified virus by centrifugation and fragmented by alkali treatment. The poly(A)-containing, 3'-derived fragments were end labeled and isolated by oligo(dT)-cellulose chromatography before they were size fractionated by agarose-urea gel electrophoresis. After electrophoresis, transversal slices of the gel were counted. The arrows indicate the positions of the virus-specific intracellular RNA species 4, 5, 6, and 7, which were run as markers in the same gel.

DISCUSSION

We have shown in this study that RNA 1 present in MHV-A59-infected cells is indeed the intracellular form of the genome. We cannot exclude, however, that there are minor differences between the genome and the fraction of RNA 1 that is present in polyribosomes since this fraction comprises only 10% of RNA 1, and minor differences might go unnoticed because of the complexity of the RNase T_1 oligonucleotide fingerprint of the genome. We did not detect differences between our T_1 oligonucleotide fingerprints of the genome or RNA 1 and those described by Lai and Stohlman (7). It was impossible, however, to correlate our fingerprint of the genome of MHV-A59 with that described by Wege et al. (17).

Our results show that RNAs 1, 3, 6, and 7 and presumably all other MHV-A59-specific RNAs form a nested set. This is in agreement with the situation for infectious bronchitis virus (14) and with the findings of Weiss and Leibowitz (18) and Cheley et al. (1) that cDNA prepared against the 3' end of the genome of MHV-A59 or RNA 7 annealed with all other MHV-A59-specific RNAs. We found that all of the RNA 7-specific T_1 oligonucleotide spots were also present in RNAs 1, 3, and 6. With the exception of one oligonucleotide spot, those in RNA 6 were present in RNA 3. A possible explanation for the absence of this spot in RNA 3 could be that it was derived from the capped 5' end of RNA 6. Because of the complexity of the T_1 oligonucleotide fingerprint of the genome in the region where this oligonucleotide was located, it was not possible to determine whether this spot also lacked in a fingerprint from the genome or RNA 1. Very recently, Lai et al. (6) and Leibowitz et al. (9) described studies in which they showed by RNase T_1 oligonucleotide fingerprinting that the MHV-A59-specific RNAs form a nested set. There are only minor differences between these T_1 oligonucleotide fingerprints of RNAs 1, 3, 6, and 7 and those described by us.

We (11) and others (12) have demonstrated that the subgenomic mRNAs 3, 6, and 7 act monocistronically. It was postulated before, and it is clear now, that these mRNAs have a unique 5' region; the size of the translation products of the mRNAs corresponds to the theoretical values expected if this 5' unique region of each mRNA species would be translated. Apparently, the internal initiation sites present in the RNAs remain cryptic.

Upon entering the cell, the infectious genome is probably first translated into RNA polymerase molecules which then recognize the 3' end of the genome and synthesize a number of negative-stranded templates. Since our data indicate that the 3' end of the genome and those of the

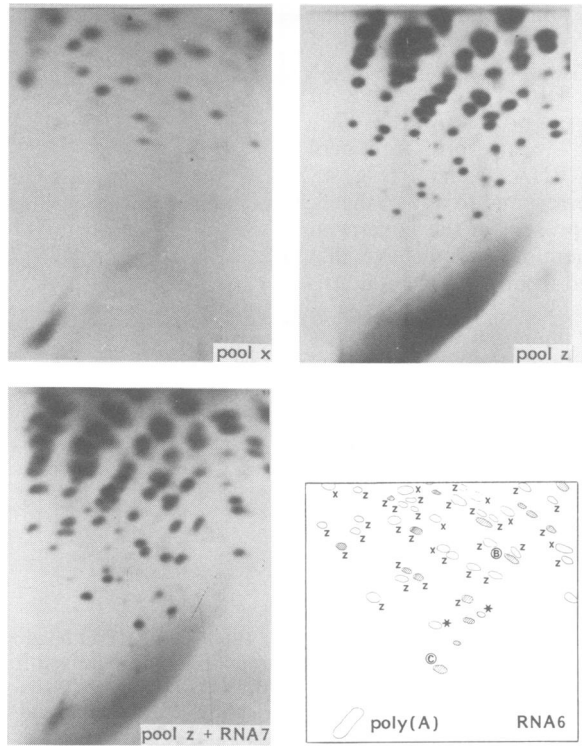

FIG. 4. RNase T_1 oligonucleotide fingerprints of RNA pools x and z and a mixture of pool z and RNA 7. Pools x and z consisted of 3'-terminal fragments of the genome; they were digested with RNase T_1, kinase labeled, and fingerprinted. In one experiment RNase T_1 oligonucleotides of in vivo ^{32}P-labeled RNA 7 were mixed with the kinase-labeled T_1 oligonucleotides of pool z and fingerprinted together. The results are summarized in a schematic drawing of the lower part of the T_1 map of RNA 6 in which C and B indicate the positions of the xylene cyanol FF and bromophenol blue tracker dyes, respectively. The open spots in the scheme represent those present in both RNA 7 and RNA 6, whereas the cross-hatched spots are those unique for RNA 6. The significance of the two spots marked with an asterisk is discussed in the text.

mRNAs are apparently identical, there should be some mechanism to prevent the RNA polymerase molecules from transcribing the mRNAs later on in infection when they are far more numerous than the negative-stranded templates.

We compared the T_1 oligonucleotide fingerprints of RNA 7 with a fingerprint of an RNA preparation of 3'-derived fragments of the genome having a size slightly larger than that of RNA 7 (pool z). As expected, a number of spots in both fingerprints matched perfectly. Surprisingly, however, two major spots in the fingerprint of RNA 7 were conspicuously lacking in the fingerprint of the pool z RNA fragments. The same two T_1 oligonucleotides were also present in RNAs 1, 3, and 6 and in virion RNA. This two-spot difference between the fingerprints of the virus-specific RNAs and the RNA fragments present in pool z could not be attributed to the different labeling conditions of the RNAs since the two spots in the RNA 7 fingerprint were also present after end labeling of the T_1 oligonucleotides with T_4 polynucleotide kinase (data not shown). A reasonable interpretation of these data is that the two spots are derived from a leader sequence containing 5'-proximal sequences of the genome. How could such a leader sequence arise? We have shown that the UV target sizes of the templates of the MHV-A59-specific RNAs are identical to their physical sizes (5). This implies that a leader sequence cannot possibly have originated from splicing from larger precursor molecules. There are, however, two other mechanisms by which a leader could possibly be created. (i) The leader may come from a small RNA primer that binds to the negative-stranded template. Since viral RNA synthesis is not inhibited in the presence of actinomycin D, this primer should be virus-specific. (ii) By a hitherto unknown kind of RNA polymerase jumping mechanism, newly synthesized 5'-proximal sequences could become linked to 3'-proximal sequences to yield the

mRNAs. Sequence analysis of the 5′ end of the genome and of RNA 7 or RNA 6 would give more information about the existence of such a leader sequence.

There are no indications so far for a leader sequence in the mRNAs of infectious bronchitis virus. Stern and Kennedy (15) have compared fingerprints of increasing size derived from the 3′ end of the genome of this virus with those of the mRNAs. Their data indicated that the intracellular RNA species were colinear with the genome. They could not, however, exclude small sequence rearrangements. If such sequence rearrangements are present in the case of infectious bronchitis virus, they might have been missed because they did not give rise to characteristic RNase T_1 oligonucleotide spots, or the spots may have been present at less conspicuous positions than in the case of MHV-A59.

We compared our results carefully with the RNase T_1 oligonucleotide fingerprints of MHV-A59 RNAs reported by Lai et al. (6) and Leibowitz et al. (9), which show a great degree of similarity with ours. The two oligonucleotide spots present in RNA 7 but not in the segment that was derived from the 3′ end of the genome, which is larger than RNA 7, correspond with oligonucleotide spots 10 and 19 reported by Lai et al. (6), with spot 10 being the larger one. Lai et al. (6) made fingerprints of poly(A)-containing fragments of the MHV-A59 genome of various sizes. This experiment complemented our data insofar as oligonucleotide spots 10 and 19 were lacking in fragments up to about 12 kilobases that were smaller than the genome, with the exception, however, of the smallest fragment, with a size of about 2 kilobases. We find it hard to explain this last observation.

Another interesting observation of the work of Lai et al. and Leibowitz et al. is that oligonucleotide spot 19 was not present in the fingerprints of RNA 4 (9) and RNA 5 (6, 9). Instead, for each of the RNAs a new unique spot was found. Such a finding could, e.g., be explained by the assumption that spot 19 comes from the junction between 5′ sequences and 3′ sequences which could slightly differ because of a small difference in the RNA polymerase jump.

Although this last assumption is highly speculative, its consequences can be tested in the near future. Finally, our preliminary data indicating a leader sequence in the mRNAs of MHV-A59 are also relevant for studies on the replication and transcription mechanism of the viral genome, since they might imply unusual properties of the replicative forms and replicative intermediates present in virus-infected cells.

ACKNOWLEDGMENTS

We thank M. Maas Geesteranus for the preparation of this manuscript.

This investigation was supported by the Foundation for Medical Research (FUNGO).

LITERATURE CITED

1. **Cheley, S., R. Anderson, M. J. Cupples, E. C. M. Lee Chan, and V. L. Morris.** 1981. Intracellular murine hepatitis virus-specific RNAs contain common sequences. Virology **112**:596–604.
2. **Clewley, J., J. Gentsch, and D. H. L. Bishop.** 1977. Three unique viral RNA species of snowshoe hare and La Crosse bunyaviruses. J. Virol. **22**:459–468.
3. **De Wachter, R., and W. Fiers.** 1972. Preparative two-dimensional polyacrylamide gel electrophoresis of ^{32}P-labeled RNA. Anal. Biochem. **49**:184–197.
4. **England, T. E., and O. C. Uhlenbeck.** 1978. 3′-Terminal labeling of RNA with T_4 RNA ligase. Nature (London) **275**:560–561.
5. **Jacobs, L., W. J. M. Spaan, M. C. Horzinek, and B. A. M. van der Zeijst.** 1981. Synthesis of subgenomic mRNA's of mouse hepatitis virus is initiated independently: evidence from UV transcription mapping. J. Virol. **39**:401–406.
6. **Lai, M. M. C., P. R. Brayton, R. C. Armen, C. D. Patton, C. Pugh, and S. A. Stohlman.** 1981. Mouse hepatitis virus A59: mRNA structure and genetic localization of the sequence divergence from hepatotropic strain MHV-3. J. Virol. **39**:823–834.
7. **Lai, M. M. C., and S. A. Stohlman.** 1981. Comparative analysis of RNA genomes of mouse hepatitis viruses. J. Virol. **38**:661–670.
8. **Langridge, L., P. Langridge, and P. L. Bergquist.** 1980. Extraction of nucleic acids from agarose gels. Anal. Biochem. **103**:264–271.
9. **Leibowitz, J. L., K. C. Wilhelmsen, and C. W. Bond.** 1981. The virus-specific intracellular RNA species of two murine coronaviruses: MHV-A59 and MHV-JHM. Virology **114**:39–51.
10. **Pedersen, F. S., and W. A. Haseltine.** 1980. Analysis of the genome of an endogenous, ecotropic retrovirus of the AKR strain of mice: micromethod for detailed characterization of high-molecular-weight RNA. J. Virol. **33**:349–365.
11. **Rottier, P. J. M., W. J. M. Spaan, M. C. Horzinek, and B. A. M. van der Zeijst.** 1981. Translation of three mouse hepatitis virus strain A59 subgenomic RNAs in *Xenopus laevis* oocytes. J. Virol. **38**:20–26.
12. **Siddell, S. G., H. Wege, A. Barthel, and V. ter Meulen.** 1980. Coronavirus JHM: cell-free synthesis of structural protein p60. J. Virol. **33**:10–17.
13. **Spaan, W. J. M., P. J. M. Rottier, M. C. Horzinek, and B. A. M. van der Zeijst.** 1981. Isolation and identification of virus-specific mRNAs in cells infected with mouse hepatitis virus (MHV-A59). Virology **108**:424–434.
14. **Stern, D. F., and S. I. T. Kennedy.** 1980. Coronavirus multiplication strategy. I. Identification and characterization of virus-specific RNA. J. Virol. **34**:665–674.
15. **Stern, D. F., and S. I. T. Kennedy.** 1980. Coronavirus multiplication strategy. II. Mapping the avian infectious bronchitis virus intracellular RNA species to the genome. J. Virol. **36**:440–449.
16. **Wege, H., S. Siddell, M. Sturm, and V. ter Meulen.** 1981. Coronavirus JHM: characterization of intracellular viral RNA. J. Gen. Virol. **54**:213–217.
17. **Wege, H., J. R. Stephenson, M. Koga, H. Wege, and V. ter Meulen.** 1981. Genetic variation of neurotropic and non-neurotropic murine coronaviruses. J. Gen. Virol. **54**:67–74.
18. **Weiss, S. R., and J. L. Leibowitz.** 1981. Comparison of the RNAs of murine and human coronaviruses, p. 245–259. *In* V. ter Meulen, S. G. Siddell, and H. Wege (ed.), Biochemistry and biology of coronaviruses. Plenum Press, New York.